Journal of Solid State Chemistry 183 (2010) 1114–1119

Contents lists available at ScienceDirect

Journal of Solid State Chemistry

journal homepage: www.elsevier.com/locate/jssc

Synthesis and selective IR absorption properties of iminodiacetic-acid intercalated MgAl-layered double hydroxide

Lijing Wang, Xiangyu Xu, David G. Evans, Xue Duan, Dianqing Li *

State Key Laboratory of Chemical Resource Engineering, Beijing University of Chemical Technology, The College of Science, Number 15 , Beisanhuandonglu, Box 98, Beijing 100029, China

ARTICLE INFO

Article history:
Received 9 November 2009
Received in revised form
6 March 2010
Accepted 14 March 2010
Available online 18 March 2010

Keywords:
Layered double hydroxide
Intercalation
Iminodiacetic acid
Selective IR adsorption
Polyethylene film

ABSTRACT

An MgAl-NO_3-layered double hydroxide (LDH) precursor has been prepared by a method involving separate nucleation and aging steps (SNAS). Reaction with iminodiacetic acid (IDA) under weakly acidic conditions led to the replacement of the interlayer nitrate anions by iminodiacetic acid anions. The product was characterized by XRD, FT-IR, TG-DTA, ICP, elemental analysis and SEM. The results show that the original interlayer nitrate anions of LDHs precursor were replaced by iminodiacetic acid anions and that the resulting intercalation product MgAl-IDA-LDH has an ordered crystalline structure. MgAl-IDA-LDH was mixed with low density polyethylene (LDPE) using a masterbatch method. LDPE films filled with MgAl-IDA-LDH showed a higher mid to far infrared absorption than films filled with MgAl-CO_3-LDH in the 7–25 μm range, particularly in the key 9–11 μm range required for application in agricultural plastic films.

1. Introduction

The growth of crops requires solar energy. The sun supplies the crops with solar energy during the day but the heat generated by the sunlight will be rapidly lost at night. The wavelengths of heat radiation energy emitted from the earth's surface to the atmosphere at night range from 7 to 25 μm (1428–400 cm^{-1}), with the peak being in the range 9–11 μm (1111–909 cm^{-1}) in the mid infrared region. Polymers such as low density polyethylene (LDPE) are widely used in agricultural plastic films in greenhouses, and the worldwide demand for plastic agricultural films reached 3.6 million tones in 2008. The heat retention properties of LDPE film may be enhanced by incorporating an inorganic material such as talc or china clay as an infrared absorbent [1–3]. However, these substances often contain impurities which promote degradation of the film. Their variable particle size also has an adverse effect on the stability of the film and has the additional disadvantage of reducing transmission of visible light and thermal short wavelength infrared radiation during the day. There is therefore a need to develop synthetic materials with high purity and controllable particle size as alternative inorganic fillers for use in agricultural plastic films.

Layered double hydroxides (LDHs) are a class of anionic clays whose general formula is $[M^{2+}_{1-x}M^{3+}_{x}(OH)_2]^{x+}(A^{n-})_{x/n}\cdots mH_2O$, where M^{2+} and M^{3+} represent divalent and trivalent cations, respectively [4–6]. The interlayer anion (A^{n-}) may be varied over a wide range and the value of the stoichiometric coefficient (x) should generally be between 0.2 and 0.33 in order to obtain pure LDH phases. The laminar structure of LDHs and high charge density of their sheets are responsible for their anionic exchange and intercalation abilities which give them extremely varied potential technological applications in fields such as catalysis, electrochemistry, separation technology and medicine [7–10]. We have developed a new method for the synthesis of LDHs involving separate nucleation and aging steps [11,12], which has the advantage of giving materials with a much narrower range of particle size than can be obtained by conventional coprecipitation. As a result, when the material is incorporated in an LDPE film, the transmission of visible light and thermal short wavelength infrared radiation is higher than in films containing fillers with a wide range of particle size. MgAl-CO_3-LDHs strongly absorb infrared radiation in the range 7–8 μm (1428–1250 cm^{-1}), associated with the ν_3 vibrational mode of the carbonate anion, and is therefore used as an infrared absorbing filler in LDPE films [13–15]. It is far from ideal, however, because it is transparent at the wavelengths where the amount of radiant heat is a maximum.

In order to increase the efficiency of LDHs as a filler, it should be possible to take advantage of their anionic exchange ability to incorporate anions which have strong infrared absorption in the required range. Iminodiacetic acid (IDA) is a white crystalline substance used as an intermediate in the manufacture of chelating agents, surface-active agents, and complex salts, and is cheap and readily available. The chemical structural formula of IDA is shown in Fig. 1.

* Corresponding author. fax: +8610 6442 5385.
E-mail addresses: lidq@mail.buct.edu.cn, dianqingli@163.com (D. Li).

0022-4596/$ - see front matter © 2010 Elsevier Inc. All rights reserved.
doi:10.1016/j.jssc.2010.03.022

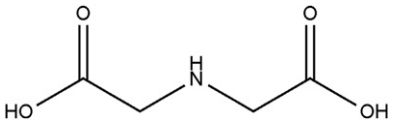

Fig. 1. The chemical structural formula of IDA.

IDA ($C_4H_7NO_4$) shows strong and broad infrared absorption in the range 1800–900 cm^{-1} by virtue of the presence of the C–N, N–H and COOH groups. So we decided to investigate the performance of LDHs containing iminodiacetic acid (IDA) anions as selective IR absorbing agents.

In this work, we use MgAl-NO_3-LDHs prepared by the method of separate nucleation and aging steps [11,12] as a precursor, in order to take advantage of the much narrower range of particle size of the material prepared using this method. Reaction of an MgAl-NO_3-LDH precursor with IDA anions was carried out under mildly acidic conditions. The resulting MgAl-IDA-LDH product was dispersed in LDPE and fabricated into MgAl-IDA-LDH/LDPE films. The infrared absorbing ability of the film was compared with LDPE film containing MgAl-CO_3-LDH.

2. Experimental section

2.1. Chemicals

$Mg(NO_3)_2\cdots 6H_2O$, $Al(NO_3)_3\cdots 9H_2O$, NaOH and Na_2CO_3 were all of A.R. grade. Iminodiacetic acid ($C_4H_7NO_4$) was C.P. grade purchased from Sinopharm Chemical Reagent Co. Ltd. Low density polyethylene (LDPE) resin 1I2A was purchased from China Sinopec Yanshan Chemical Corporation. Deionized water was used in all experiments and it had a conductivity of less than 10^{-6} S cm^{-1}.

2.2. Preparation of MgAL-NO_3-LDH precursor

An aqueous mixed salt solution containing Mg^{2+} and Al^{3+} was prepared with Mg/Al molar ratio of 2.0 in which the concentration of Mg^{2+} was 0.8 mol L^{-1}. An aqueous mixed base solution containing NaOH was prepared with $n(NaOH)/[n(Mg^{2+})+n(Al^{3+})]=2.0$. The mixed salt solution was mixed with the base solution in a modified colloid mill reactor following the procedure developed in our laboratory [11,12,16]. The resulting slurry was aged at reflux temperature for 6 h. The precipitate was then filtered, and washed until the washings reached pH ~ 7. Some wet filter cake was set aside for the preparation of MgAl-IDA-LDH and the remainder was dried in a desiccator to afford MgAl-NO_3-LDH powder. This process allowed the amount of solid in the wet cake to be estimated.

2.3. Preparation of MgAl-IDA-LDH

IDA (5.3 g, 0.04 mol) was dissolved in deionized water, from which the CO_2 had been removed by boiling and then cooling under nitrogen. The pH value of the solution was adjusted to around 4.2 by the addition of NaOH. The wet cake of MgAl-NO_3-LDH (35.2 g, calc. 0.02 mol of NO_3^-) was dispersed in deionized water and added dropwise into the reactor, with the pH being maintained at 4.5 during the whole reaction. The resulting slurry was aged at reflux temperature for 6 h. The reaction was carried out under a stream of N_2. The precipitate was then filtered, washed and dried in a desiccator to obtain the MgAl-IDA-LDH powder.

2.4. Preparation of MgAl-CO_3-LDH

In order to compare the infrared absorption ability of MgAl-IDA-LDH with that of MgAl-CO_3-LDH, MgAl-CO_3-LDH was prepared. An aqueous mixed salt solution containing Mg^{2+} and Al^{3+} was prepared with Mg/Al molar ratio of 2.0 in which the concentration of Mg^{2+} was 0.8 mol L^{-1}. An aqueous mixed base solution containing NaOH and Na_2CO_3 was prepared with $n(CO_3^{2-})/n(Al^{3+})=2$ and $n(NaOH)/[n(Mg^{2+})+n(Al^{3+})]=1.6$. The mixed salt solution was mixed with the base solution in a modified colloid mill reactor following the procedure developed in our laboratory [11,12,16]. The resulting slurry was aged at reflux temperature for 6 h. The precipitate was then filtered, washed and dried in a desiccator to obtain the MgAl-CO_3-LDH powder.

2.5. Preparation of LDH/LDPE films

MgAl-IDA-LDH and MgAl-CO_3-LDH were mixed with LDPE in a double-roller mixer, with the final content of LDHs fixed at 4 wt.%. In order to disperse LDHs in LDPE uniformly, masterbatch technology was used: 4 g of LDPE granules and 3 g of LDHs were blended in double-roller mixer for 15 min at 130 °C to give a masterbatch. 1.4 g of the masterbatch was then blended with 13.6 g of LDPE for 5 min at 130 °C. The resulting composites were then moulded at 160 °C into films with a thickness of 100 μm.

2.6. Analysis and characterization

Powder X-ray diffraction (XRD) patterns were recorded on a Shimadzu XRD-6000 powder X-ray diffractometer (Cu Kα radiation, $\lambda=0.15406$ nm) between 3° and 70° with a scan speed of 5° min^{-1}. FT-IR spectra were recorded on a Bruker Vector 22 spectrometer using the KBr pellet technique (sample/KBr = 1/100 weight ratio) in the range 4000–400 cm^{-1} at a resolution of 2 cm^{-1}. The compositions of Mg and Al in samples were determined with a Shimadzu ICPS-7500 inductively coupled plasma (ICP) emission spectrometer using solutions prepared by dissolving the samples in dilute HNO_3 and the content of carbon and nitrogen was determined using a Elementar Vario EI elemental analyzer. Thermogravimetry and differential thermal analysis (TG-DTA) curves were obtained on an HCT-2 instrument in the temperature range 60–650 °C with a heating rate at 10 °C min^{-1} in air. The morphology of the LDH particles was examined by scanning electron microscopy (SEM) using a Hitachi S-4700 microscope. A Hitachi H-800 transmission electron microscope (TEM) was used to observe the dispersion of LDH fillers in LDPE. The LDH/LDPE composite was microtomed as very thin slices using a cryo-microtome in liquid nitrogen and then imaged by TEM.

2.7. Infrared absorbance and visible light transmittance tests

The infrared absorbance was recorded on a Bruker Vector 22 instrument. The average transmittance over different wavelength ranges was calculated by the integration method. The visible light transmittance was recorded using a Shimadzu UV-2501PC instrument in the wavelength range 380–780 nm using air as reference. The average transmittance was calculated by the integration method.

3. Results and discussion

3.1. Structure and morphology of MgAl-NO_3-LDH and MgAl-IDA-LDH

The powder XRD patterns of MgAl-NO_3-LDH and MgAl-IDA-LDH are shown in Fig. 2. The XRD pattern of the MgAl-NO_3-LDH precursor (Fig. 2a) exhibited the typical reflections of an LDH phase. The (003) and (006) diffraction peaks, which correspond to the basal and higher order reflections, appeared at 10.07° and 20.11°, respectively. The basal distance d(003) was 0.88 nm, which is within the range of values reported in the literature (0.81–0.89 nm) [17,18]. After IDA anions were intercalated into the interlayer galleries of MgAl-NO_3-LDH, the new (003), (006) and (009) diffraction peaks moved to 7.19°, 14.50° and 21.90°, respectively, as shown in Fig. 2b. The corresponding basal distance of d(003) was 1.23 nm, which suggests that the larger IDA anions have replaced the NO_3^- in the interlayer galleries to form MgAl-IDA-LDH. Furthermore, the diffraction peak near 61.1° corresponding to the (110) reflection of the two samples showed no significant shift in position. The strong sharp reflections indicate that the MgAl-IDA-LDH had a well-formed layered crystalline structure.

SEM images of MgAl-NO_3-LDH and MgAl-IDA-LDH are shown in Fig. 3. Both MgAl-NO_3-LDH and MgAl-IDA-LDH have the plate-like morphology typical of LDHs. The size of the primary particles of MgAl-NO_3-LDH ranges from 50 to 200 nm and only a limited extent of aggregation of the particles can be observed. The size of the MgAl-IDA-LDH particles also ranges from 50 to 200 nm, and the shape and grain size show no significant change after anion exchange, showing that the size distribution induced by the separate nucleation and aging steps method was retained.

3.2. TG-DTA analysis of MgAl-NO_3-LDH and MgAl-IDA-LDH

TG and DTA curves of MgAl-NO_3-LDH and MgAl-IDA-LDH are shown in Fig. 4. MgAl-NO_3-LDH showed two weight loss steps with increasing temperature. The first step observed at 60–237 °C corresponds to the removal of surface adsorbed and interlayer crystal water, the associated weight loss was 6.7%. A second weight loss step at 237–568 °C can be attributed to dehydroxylation of the layers, decomposition of the interlayer nitrate anions and collapse of layer structure; the associated weight loss was 36.1%. There were three endothermic peaks in the DTA curve. The endothermic peak at 130 °C corresponds to the removal of interlayer water, and the two peaks at 360 and 498 °C result from dehydroxylation and decomposition of interlayer nitrate anions.

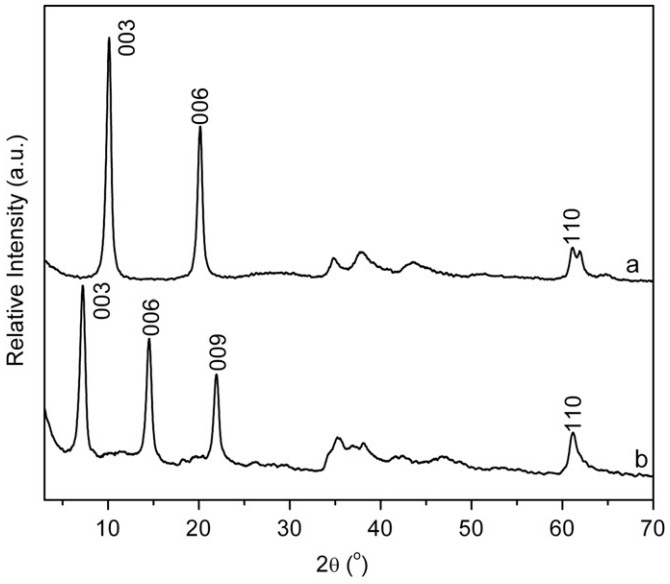

Fig. 2. Powder XRD patterns of (a) MgAl-NO_3-LDH and (b) MgAl-IDA-LDH.

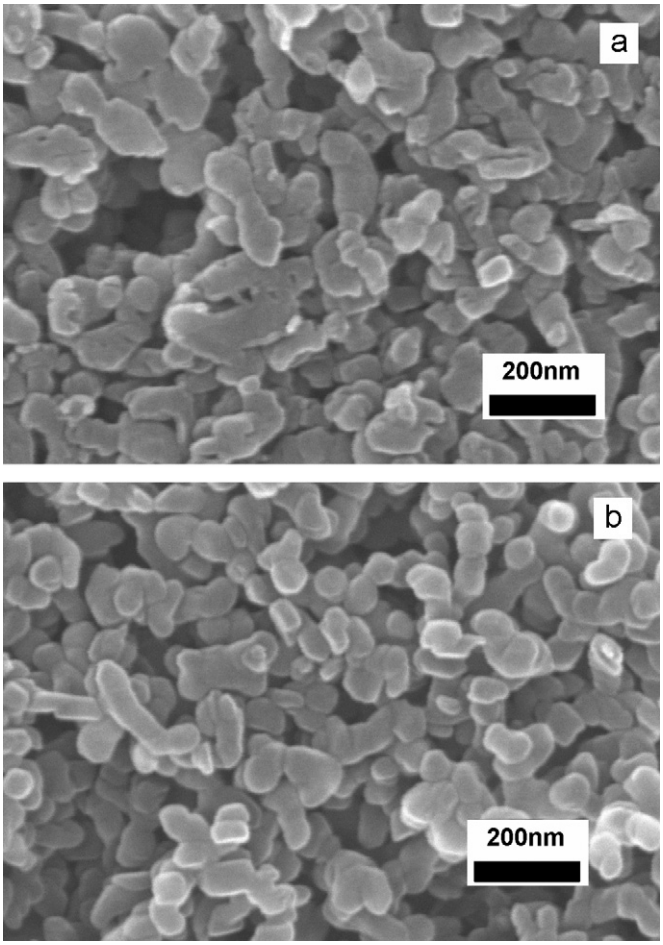

Fig. 3. SEM images of (a) MgAl-NO_3-LDH and (b) MgAl-IDA-LDH.

MgAl-IDA-LDH showed two weight loss steps with increasing temperature. The first step at 60–240 °C responds to the removal of surface adsorbed and interlayer crystal water; the associated weight loss was 6.0%. The second weight loss step at 240–576 °C can be attributed to dehydroxylation of the layers, decomposition and combustion of interlayer iminodiacetic acid and collapse of the layer structure; the associated weight loss was 25.1%. There were two endothermic peaks and two exothermic peaks in the DTA curve. The weak endothermic peaks at about 122 and 192 °C corresponds to the removal of surface adsorbed and interlayer water, and the exothermic peaks at about 342 and 429 °C result from decomposition and combustion of iminodiacetic acid anions.

3.3. Analysis of the chemical composition of MgAl-NO_3-LDH and MgAl-IDA-LDH

The results of elemental analysis and the calculated structural formulae of the MgAl-NO_3-LDH precursor and MgAl-IDA-LDH are listed in Table 1. The results confirm that nitrate anions in the precursor have been completely replaced by iminodiacetate anions. The quantities of water were determined according to the first weight loss step in the TG curves. The molar ratio of Mg/Al in the layers was essentially unchanged, indicating that there was no destruction of the layers during the anion exchange

process; this is consistent with the XRD analysis. For MgAl-NO_3-LDH and MgAl-IDA-LDH, the TG weight loss observed in each stage is consistent with the expected amount of species lost on the basis of the calculated structural formulae.

3.4. TEM micrographs of LDH/LDPE composites

TEM was performed in order to determine the degree of dispersion of LDHs particles inside the polymer matrix. The TEM micrograph for MgAl-IDA-LDH and MgAl-CO_3-LDH in LDH/LDPE containing 4 wt.% of MgAl-IDA-LDH and MgAl-CO_3-LDH are shown in Fig. 5. The dark areas represent the LDHs and the gray-white areas represent the polymer matrices. These low magnification images provide a clear indication that the LDHs particle dispersion is on the nano-scale, and discrete LDHs particles can be detected throughout the matrix; these particles are either individual primary particles or clusters of the primary particles. In general, all the LDHs exhibited good dispersion within the polymer matrix.

3.5. FT-IR analysis and infrared absorption of LDHs and LDH/LDPE film samples

FT-IR spectra of MgAl-NO_3-LDH, MgAl-IDA-LDH and MgAl-CO_3-LDH samples are shown in Fig. 6. The spectra show the

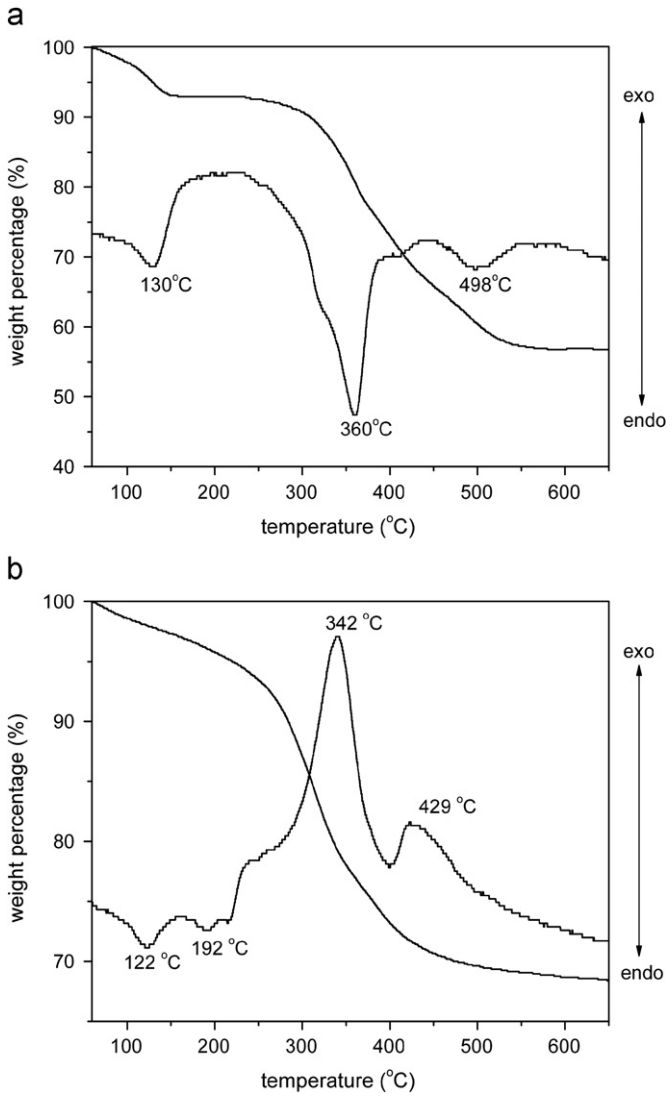

Fig. 4. TG-DTA curves of (a) MgAl-NO_3-LDH and (b) MgAl-IDA-LDH.

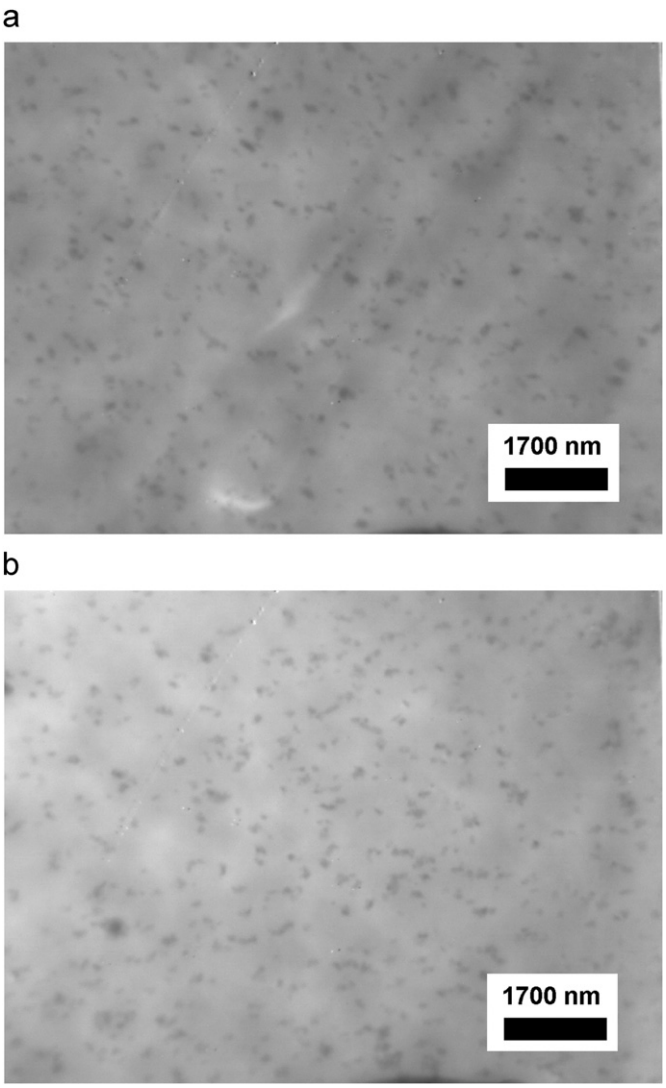

Fig. 5. TEM photographs of LDH/LDPE composites with 4 wt.% loadings of (a) MgAl-IDA-LDH and (b) MgAl-CO_3-LDH.

Table 1
Chemical compositions of MgAl-NO_3-LDH and MgAl-IDA-LDH.

Sample	Mg Found (calc.)	Al Found (calc.)	C Found (calc.)	N Found (calc.)	H_2O Found (calc.)	Formula
MgAl-NO_3-LDH	19.27 (19.39)	10.36 (10.28)	0 (0)	5.32 (5.34)	6.7 (6.6)	$Mg_{0.677}Al_{0.323}(OH)_2(NO_3^-)_{0.323}\cdot 0.31H_2O$
MgAl-IDA-LDH	19.21 (19.31)	10.13 (10.18)	8.98 (9.06)	2.73 (2.64)	6.0 (5.9)	$Mg_{0.678}Al_{0.322}(OH)_2(C_4H_5NO_4^{2-})_{0.161}\cdot 0.28H_2O$

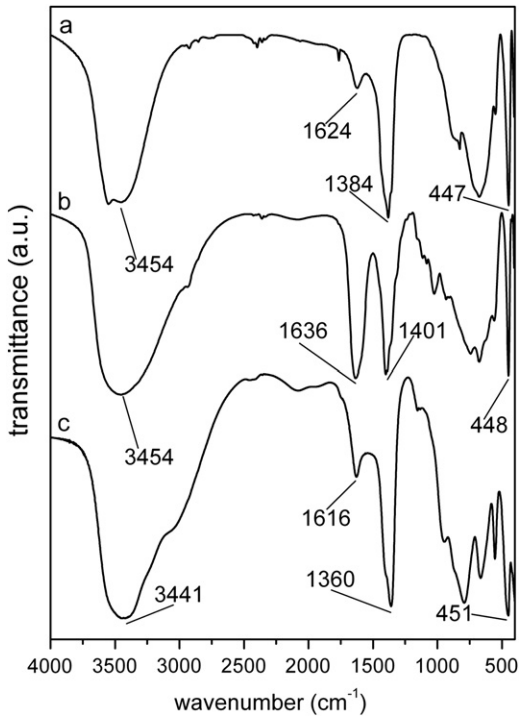

Fig. 6. FT-IR spectra of (a) MgAl-NO_3-LDH, (b) MgAl-IDA-LDH and (c) MgAl-CO_3-LDH.

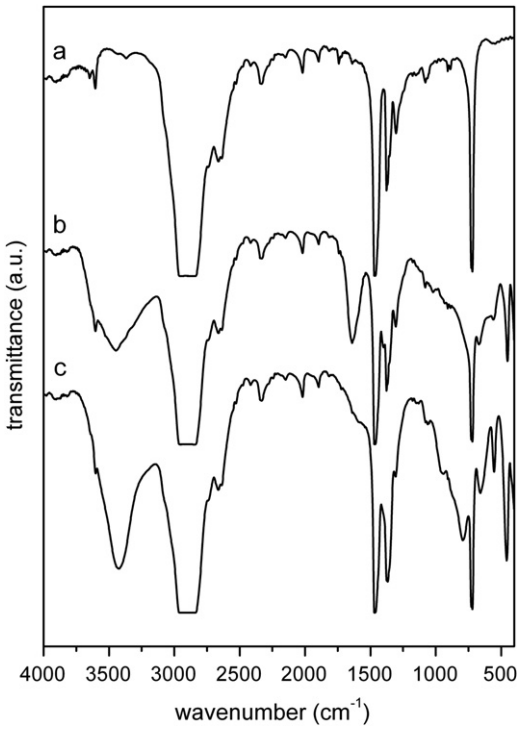

Fig. 7. FT-IR spectra of (a) LDPE reference film, (b) MgAl-IDA-LDH/LDPE film and (c) MgAl-CO_3-LDH/LDPE film.

typical infrared absorption characteristics of LDHs. The broad peak around 3450 cm^{-1} in Figs. 6a–c can be ascribed to the stretching vibration of OH groups attached to Al or Mg in the layers. The band at about 1624 cm^{-1} can be attributed to the deformation vibration of water molecules in the interlayer domain. The absorption band at about 447 cm^{-1} can be assigned to the vibration of O–M–O units in the layers [19]. In addition to these bands, the spectrum of MgAl-NO_3-LDH in Fig. 6a shows the characteristic sharp absorption band of the ν_3 stretching vibration of NO_3^- at about 1384 cm^{-1} [20]. After intercalation of iminodiacetate anions in LDH (Fig. 6b), the bands at about 1714 cm^{-1} of the stretching vibration of C=O in IDA shifted to lower frequency (1636 and 1401 cm^{-1}), confirming that the –COOH groups had been converted into $-COO^-$ after intercalation. The absorption peak at 1636 and 1401 cm^{-1} are attributed to the asymmetric stretching vibration and symmetric stretching vibrations, respectively, of $-COO^-$ [21,22]. The absorption band of the NO_3^- anion disappeared, indicating that replacement of NO_3^- by iminodiacetate anions was complete. The spectrum of MgAl-CO_3-LDH in Fig. 6c shows the characteristic sharp absorption band of the asymmetric stretch of CO_3^{2-} at about 1360 cm^{-1}.

FT-IR spectra of the LDPE film, MgAl-IDA-LDH/LDPE film and MgAl-CO_3-LDH/LDPE film samples are shown in Fig. 7.

Films filled with LDHs have distinctly superior infrared absorbing ability in the 1428–400 cm^{-1} range compared with the LDPE reference film. The values of average transmittance over different wavenumber ranges are shown in Table 2. The reduction in the value of average transmittance in different wavenumber ranges of MgAl-IDA-LDH/LDPE film (as a percentage of the value of the MgAl-CO_3-LDH/LDPE film) were calculated and are also shown in Table 2.

The MgAl-IDA-LDH/LDPE film showed clearly superior infrared absorption compared with the MgAl-CO_3-LDH/LDPE film in both the wider 1428–400 cm^{-1} and narrower 1428–714 cm^{-1} ranges, and especially in the key 1111–909 cm^{-1} range in which the amount of heat radiated from the earth's surface to the atmosphere is maximum. This shows that MgAl-IDA-LDH/LDPE has appropriate IR absorption properties to be used in agricultural plastic films.

3.6. Visible light transmittance of LDH/LDPE films

Visible light provides energy for plant photosynthesis and the visible light transmittance of agricultural films is therefore important. The visible light transmittance curves of LDPE film, MgAl-IDA-LDH/LDPE film and MgAl-CO_3-LDH/LDPE film in the visible light wavelength range 380–780 nm are shown in Fig. 8.

The average transmittances were calculated by the integration method and the results are shown in Table 3. It can be seen from Table 3 that there was only a very small reduction in visible light transmittance when LDH was incorporated in the film, showing that its inclusion in the film would not have an adverse effect on plant growth.

4. Conclusions

MgAl-IDA-LDH has been prepared from an MgAl-NO_3-LDH precursor by an anion exchange reaction in a partially neutralized solution of iminodiacetic acid under a nitrogen atmosphere. XRD and ICP showed that the structure of the layers remained unchanged after the anion exchange reaction, but the interlayer spacing increased. ICP analysis and TG data showed that the final compound had the composition $Mg_{0.678}Al_{0.322}(OH)_2(C_4H_5NO_4^{2-})_{0.161}\cdots 0.28H_2O$. An MgAl-IDA-LDH/LDPE film showed higher infrared absorption than an MgAl-CO_3-LDH/LDPE film in both the wider 1428–400 and narrower 1428–714 cm^{-1} ranges, and especially in the 1111–909 cm^{-1} range in which the amount of heat radiated from the earth's surface to the atmosphere is a maximum. This indicates that MgAl-IDA-LDH/LDPE has

Table 2
Average transmittance (%) of MgAl-IDA-LDH/LDPE film in different wavenumber ranges and the reduction in transmittance (%) compared with that of MgAl-CO_3-LDH/LDPE film.

Sample	1428–714 cm^{-1}		1428–400 cm^{-1}		1111–909 cm^{-1}	
	Average transmittance	Transmittance reduction (%)	Average transmittance	Transmittance reduction (%)	Average transmittance	Transmittance reduction (%)
LDPE film	55.5	–	61.0	–	62.4	–
MgAl-IDA-LDH/LDPE film	40.4	5.0	40.4	6.9	45.8	10.2
MgAl-CO_3-LDH/LDPE film	42.3	0	43.4	0	51.0	0

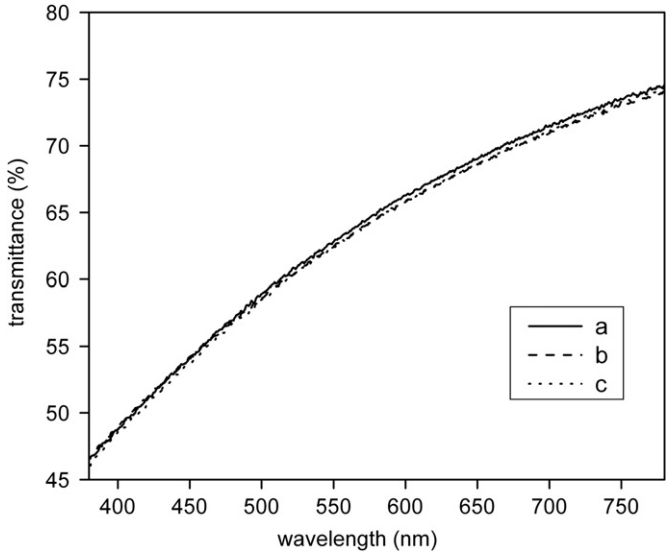

Fig. 8. Visible light transmittance curves of (a) LDPE reference film, (b) MgAl-IDA-LDH/LDPE film and (c) MgAl-CO_3-LDH/LDPE film.

Table 3
Average transmittances of LDPE and LDH/LDPE films in the range 380–780 nm.

Sample	380–780 nm Average transmittance (%)
LDPE film	63.4
MgAl-IDA-LDH/LDPE film	63.1
MgAl-CO_3-LDH/LDPE film	63.1

appropriate IR absorption properties to be used in agricultural plastic films. The addition of LDHs had little impact on the visible light transmittance of LDPE films.

Acknowledgments

This work was supported by the National Natural Science Foundation, 111 Project and Program for Changjiang Scholars and Innovative Research Team in University.

References

[1] S.Z. Wang, X. Zhao, S.C. Li, Plastics Sci. Technol. 3 (2003) 29–31 34.
[2] Y.J. Liu, Plastics Sci. Technol. 2 (2002) 22–26.
[3] Y. Tian, China Plastics 18 (2004) 1–8.
[4] J.T. Kloprogge, R.L. Frost, Appl. Catal. A-Gen. 184 (1999) 61–71.
[5] V.R.L. Constantino, T.J. Pinnavaia, Inorg. Chem. 34 (1995) 883–892.
[6] F. Kooli, K. Kosuge, T. Hibino, A. Tsunashima, J. Mater. Sci. 28 (1993) 2769–2773.
[7] S. Sasaki, S. Aisawa, H. Hirahara, A. Sasaki, H. Nakayama, E. Narita, J. Solid State Chem. 179 (2006) 1129–1135.
[8] H. Zhang, R. Qi, D.G. Evans, X. Duan, J. Solid State Chem. 177 (2004) 772–780.
[9] M. Jakupca, P.K. Dutta, Chem. Mater. 7 (1995) 989–994.
[10] K.M. Tyner, S.R. Schiffman, E.P. Giannelis, J. Control. Release 95 (2004) 501–514.
[11] Y. Zhao, F. Li, R. Zhang, D.G. Evans, X. Duan, Chem. Mater. 14 (2002) 4286–4291.
[12] Y.J. Feng, D.Q. Li, C.X. Li, Z.H. Wang, D.G. Evans, X. Duan, Clay. Clay Miner. 51 (2003) 566–569.
[13] G.Z. Xu, C.X. Guo, X. Duan, JC.G. iang, Chin. J. Appl. Chem. 16 (1999) 45–48.
[14] J.T. Kloprogge, L. Hickey, R.L. Frost, Appl. Clay Sci. 18 (2001) 37–49.
[15] Q.Z. Jiao, Y. Zhao, H. Xie, D.G. Evans, X. Duan, Chin. J. Appl. Chem. 19 (2002) 1011–1013.
[16] X. Duan, Q.Z. Jiao, F. Li, J. He, C.X. Guo, Chinese Patent, CN 00132145.5, 2000.
[17] F. Cavani, F. Trifiro, A. Vaccari, Catal. Today 11 (1991) 173–301.
[18] J.C. Villegas, O.H. Giraldo, K. Laubernds, S.L. Suib, Inorg. Chem. 42 (2003) 5621–5631.
[19] N. Iyi, T. Matsumoto, Y. Kaneko, K. Kitamura, Chem. Mater. 16 (2004) 2926–2932.
[20] S.C. Guo, D.Q. Li, W.F. Zhang, M. Pu, D.G. Evans, X. Duan, J. Solid State Chem. 177 (2004) 4597–4604.
[21] H.R. Dong, Instrumental Analysis, Chemical Industry Press, Beijing, 2000.
[22] L.Y. Zhang, Y.J. Lin, Z.J. Tuo, D.G. Evans, D.Q. Li, J. Solid State Chem. 180 (2007) 1230–1235.